Quantum-Classical Hybrid Approach for COVID-19 Severity Classification from Chest CT Images

Prabhakar Singh [a], Shashidhar Ram Joshi [b]

[a] *Department of Electronics and Computer Engineering, Pulchowk Campus, IOE, Tribhuvan University, Nepal*
✉   [a] 078msdsa013.prabhakar@pcampus.edu.np, [b] srjoshi@ioe.edu.np

Abstract

COVID-19 has significant worldwide effects in the areas of social, medical, and economy.Because of the severe effects of a disease that causes lung damage and increases susceptibility to lung infections in the population, the World Health Organization declared a Public Health Emergency of International Concern.In order to prioritize life-saving care, it is imperative to identify and evaluate the severity of COVID-19 infection in relation to other respiratory illnesses. Specialists may deploy resources more effectively and help patients in emergencies sooner when they do effective evaluations.In expert-evaluated COVID-19 CT lung images, ground glass opacity is frequently observed. Innovative methods for medical image analysis might be made possible by quantum computing's promise to explore quantum machine learning (QML).In this study,the features are extracted by using quantum ,with the abundance of data, machine learning benefits from enhanced speed and computational complexity to handle larger weight matrices for improving performance.Exploring quantum techniques for severity classification in machine learning using a Quantum-Classical hybrid model on varied input image sizes (28x28, 32x32, 64x64) running on a simulator.The patient's CT images are classified by the Quantum-Classical model into three severity classes: Critical, Severe, and Moderate. The paper demonstrates that a hybrid model outperforms CNN, achieving 96.82% accuracy with smaller 32x32 images and 3075 trainable parameters compared to VGG-19, which achieves 85.97% accuracy with larger 64x64 images and 262,659 trainable parameters.

Keywords

COVID-19, Severity, Chest CT images, Accuracy, ROC, Quantum-Classical

1. Introduction

COVID-19, caused by SARS-CoV-2, emerged in late 2019, marking the seventh coronavirus to infect humans and triggering a global health emergency [1]. As of April 8, 2024, Worldometers global real-time statistics show that there were 704,686,750 confirmed COVID-19 cases worldwide, surpassing the 704.68 million threshold. 7,009,958 fatalities overall, or 7.009 million deaths overall [2].Coronavirus spreads quickly and is especially harmful to people with pre-existing medical conditions. There is an increasing number of people affected by the post-COVID-19 condition. People who are infected with coronaviruses have difficulty breathing. Early identification of COVID-19 infection and assessment of its severity are therefore essential. By doing this, the disease's death and spread rates may be reduced.CT imaging can be used to diagnose COVID-19 ,however manual image interpretation is time-consuming and prone to human error.In order to effectively manage patients, AI-based image processing makes it possible to quickly and accurately diagnose COVID-19 from CT images. Disease monitoring and severity analysis are aided by its ability to extract complex and varied patterns from healthcare images. Treatment options might be guided by the results of sequential CT imaging, which helps to identify degree of lungs involvement. To monitor the development of the disease and provide treatment, routine follow-up scans are advised for COVID-19 patients [3, 4].

With the development of the idea of quantum-classical (QC) and its advancements in the field of machine learning (ML)

(i.e., learning capacity, run time, and learning efficiency), the QC field has demonstrated its important role in intractable problems with classical counterparts through quantum supremacy. Additionally, QC has proven to have a significant impact on machine learning with regard to near-term quantum computers [5]. In order to overcome these obstacles and enhance accuracy of models on limited datasets, quantum computing is becoming a popular computational technique [6]. Quantum models take advantage of the computer power provided by quantum mechanics to expedite drug research and help to find treatments for newly developing viruses more quickly. Traffic management is revolutionized by integrating quantum algorithms with classical traffic data. This allows for real-time optimization of signal timing to minimize traffic and boost transit efficiency.There is enormous potential for a wide range of applications with current breakthroughs in Quantum Computing, which integrate quantum and conventional computing. The current topic, which relates to the intersection of computer technology and quantum physics, uses quantum bits to give more computational capability than traditional models, particularly in machine learning [7].

Shor's method, achieving quantum supremacy, enables rapid factorization of large numbers, a task impractical for classical computers. Grover's algorithm utilizes quantum computing to search datasets efficiently, achieving $O(\sqrt{N})$ time complexity compared to traditional methods requiring at least N/2 steps [8, 9].Superposition and entanglement are used by quantum computing to outperform conventional counterparts. Advanced quantum storage relies on quantum bits, or qubits,

which are different from classical bits that are limited to either 0 or 1. Qubits can exist in a simultaneous superposition of both states 0 and 1 [10]. Hybrid quantum-classical models use the advantages of both methods to overcome the shortcomings of quantum algorithms for classification. This results in enhanced performance. Compared to high-resolution image tasks performed by CNNs, challenges such as fluctuating circuit depth, resolution and limited qubits on big datasets are reduced. In order to optimize COVID-19 severity classification of chest CT images across various classes, this research presents a unique Quantum convolution layer within a hybrid model, retaining batch sizes and quantum depths for optimal parameter adjustment.

Using textural data , such as ground-glass opacity (GGO) in the initial phase and lung consolidation taken from Computed Tomography (CT) slices, automatically categorize COVID-19 patients into three severity levels: mild, moderate, and severe [3].A two-step process involves first detecting COVID-19 and then classifying the severity into High, Moderate, or Low categories using Cubic Support Vector Machine (SVM)[11]. The method for identifying high-risk patients that was evaluated using data that was available to the public ,achieved 92% accuracy, suggesting that patient must get attention.A hybrid Quantum-Classical convolution neural network with low resolution, few trainable parameters, and a small number of training images can classify images with 93.48% accuracy [7].In order to identify COVID-19 patients using chest X-ray images, a hybrid Quantum-Classical convolutional neural network (HQ-CNN) model is proposed. It uses random quantum circuits as its foundation. The accuracy of low resolution images in binary and multiclass settings is 93.3% and 82.2%, respectively [5].Using many random quantum circuits, quanvolutional layers process the MNIST dataset. Meaningful characteristics for classification are produced via quantum transformations, which call for small quantum circuits with negligible to no error correction[12].A quantum machine learning technique classified full-image mammograms into benign and malignant groups with an 84% accuracy rate. Results from tests on simulators and quantum devices were compared with those from classical devices[10].

2. Theoretical Background

2.1 Principles of Quantum Computing

1. **Qubits**:In quantum computing, a qubit represents a bit of data and can exist in states $|0\rangle$ and $|1\rangle$ simultaneously, a phenomenon known as quantum superposition. Qubits, the fundamental units, utilize the two energy levels of an atom, with an excited state representing $|1\rangle$ and a ground state representing $|0\rangle$. These states are often depicted using bra-ket notation, also known as Dirac notation, allowing any arbitrary qubit state to be represented in a concise and standardized manner.

$$|\psi\rangle \geq \alpha|0\rangle + \beta|1\rangle \tag{1}$$

The overall state of a qubit can be visualized using Bloch spheres, representing quantum states as points on a unit sphere[13].Overall state of a qubit is represented as:

$$|\psi\rangle = \cos\left(\frac{\theta}{2}\right)|0\rangle + e^{j\psi}\sin\left(\frac{\theta}{2}\right)|1\rangle \tag{2}$$

Where θ and ψ lie within the entire sphere without any repetitions, i.e., $\theta \in [0, \pi]$ and $\psi \in [0, 2\pi]$. Here, θ represents latitude, and ψ represents longitude [7].

2. **Quantum Entanglement**:Entanglement enables quantum systems to exhibit correlated states within a superposition, allowing two particles to be linked and influence each other without direct interaction, facilitated by multi-qubit gates like the Controlled Not (C-NOT).

3. **Quantum Gates**:Out of the ten quantum gates that are available, the seven that are most frequently used in quantum computing research are used to interact with both single and multiple qubits.

- Hadamard Gate:The Hadamard gate is a sort of single-qubit gate that is used to convert base-state qubits into superposition states, which are represented by the following matrix:

$$H = \frac{1}{\sqrt{2}}\begin{bmatrix} 1 & 1 \\ 1 & -1 \end{bmatrix} \tag{3}$$

- Rotation Gates:Qubit states may be manipulated by rotating them about the basic axes, which are represented by the general formula for rotation gates in quantum computing as RY, RX, and RZ for rotations around the Y, X, and Z axes, respectively.Given is the rotation gate's generic expression:

$$R(\theta, \phi) = \begin{bmatrix} \cos(\frac{\theta}{2}) & -ie^{-i\theta}\sin(\frac{\theta}{2}) \\ -ie^{i\theta}\sin(\frac{\theta}{2}) & \cos(\frac{\theta}{2}) \end{bmatrix} \tag{4}$$

- Pauli Gates:Pauli matrices are a collection of 2×2 complex Hermitian and unitary matrices used as gates to manipulate quantum states $|\psi\rangle$ orientations in the X, Y, or Z directions.

Pauli-X gate :The X gate in quantum computing behaves similarly to a classical NOT operation by interchanging the states of the computational basis .In order for $|0\rangle$ to become $|1\rangle$ and $|1\rangle$ to become $|0\rangle$, In matrix form, Pauli X-gate is presented as:

$$X = \begin{bmatrix} 0 & 1 \\ 1 & 0 \end{bmatrix}$$

$$X = |0\rangle\langle 1| + |1\rangle\langle 0| \tag{5}$$

$$X|0\rangle = |1\rangle$$

$$X|1\rangle = |0\rangle$$

Pauli-Y gate (Y gate) : In matrix form, Pauli Y-gate is presented as:

$$Y = \begin{bmatrix} 0 & -i \\ i & 0 \end{bmatrix}$$

$$Y = i|1\rangle\langle 0| - i|0\rangle\langle 1| \tag{6}$$

$$Y = i|1\rangle\langle 0| - i|0\rangle\langle 1| \tag{7}$$

$$Y|0\rangle = +i|1\rangle$$

$$Y|1\rangle = -i|0\rangle$$

In addition to changing the qubits' state, this gate reverses their phase. **Pauli-Z gate (Z gate)** : In matrix form, Pauli Z-gate is presented as:

$$Z = \begin{bmatrix} 1 & 0 \\ 0 & -1 \end{bmatrix}$$

$$Z = |0\rangle\langle 0| - |1\rangle\langle 1| \tag{8}$$

$$Z|0\rangle = +|0\rangle$$

$$Z|1\rangle = -|1\rangle$$

Z-gates reverse the phase between the states $|0\rangle$ and $|1\rangle$ with respect to the computational basis.

4. **Quantum Measurement**:Since quantum states change into classical ones during measurements, quantum computers are probabilistic devices that require numerous observations to obtain exact results[13].This work makes use of a parameterized quantum circuit for quantum convolution and measures quantum states using the Pauli Z gate.

2.2 Quantum Deep Learning

The development of quantum deep learning and quantum-inspired approaches, investigating the possibilities of algorithms such as Grover's and Shor's in machine learning, is a result of recent developments in deep learning and quantum computing. In addition to suggesting other topologies and taking into consideration quantum circuits as an alternative to intricate CNN architectures, researchers are exploring the potential applications of quantum computing in machine learning and deep learning.

2.3 Fully Connected Layer

Fully connected layers, included in both deep learning models and conventional neural networks, are used after convolution layer outputs have been flattened. In these layers, every neuron is linked to every other neuron in the layer above. These layers incorporate linear input components and utilize activation functions to incorporate non-linearity,crucial for learning complex patterns.

A fully connected layer's functioning can be mathematically described as:

$$Output = Activation(Weight \cdot Input + Bias) \tag{9}$$

Here:

Input : The input features from the previous layer

Weight : Learnable connection parameters

Bias : The bias terms for each neuron in the layer

Activation : The activation function

2.4 Output Layer

The Softmax activation function assigns a probability to each class depending on its score in relation to the other classes, transforming a vector of scores into a probability distribution over multiple classes.

$$\sigma(z)_j = \frac{e^{z_j}}{\sum_{k=1}^{K} e^{z_k}} \quad \text{for } j = 1, \dots, K \tag{10}$$

3. Methodology

Quantum-Classical framework is used in this methodology to conduct severity classification.
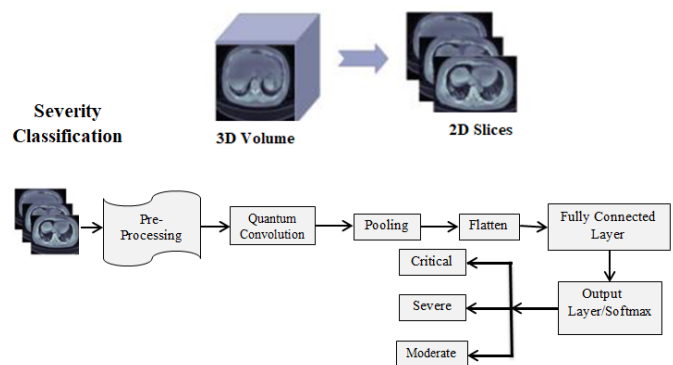

Figure 1: System Block Diagram

3.1 Dataset

The COVID-19 CT scan dataset was obtained from many sources, including Kaggle [14, 15] and Radiopaedia [16], for which different classes of severity of dataset were acquired. Researchers, doctors, and data scientists may now access a number of datasets that have been provided specifically for COVID-19 research. 120 individuals had raw CT scans in total.To complete tasks, nii formate are captured and transformed into 2D images. In order to classify severity, a total of 3975 CT images are used. The Python splitfolders package is used for train-test splits, and the split ratio for training and testing the quantum-classical model is 70:30. Additionally, to increase the number of datasets for classical deep learning, 11,050 CT images are used, with training and validation divided into 75:25.

Table 1: Dataset used for Severity classification

Class	Training	Testing	Total
Critical	942	405	1347
Severe	947	407	1354
Moderate	891	383	1274
Total	2780	1195	**3975**

Various degrees of severity are correlated with the percentage of the lung lesion area.In other reference works, patient severity was classified as either high, moderate, or low, or as either severe or non-severe; however, patient severity is classified as either moderate, severe, or critical. Ground glass opacities, in a moderate instance, 25–50 % pulmonary
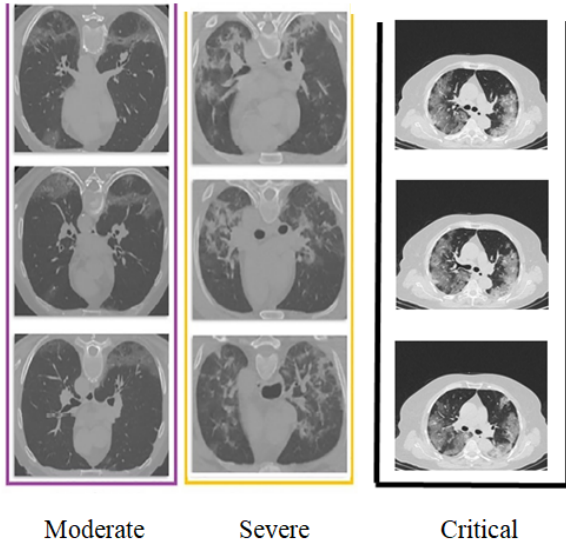
Figure 2: CT slices of Moderate,Severe and Critical COVID-19 cases

parenchymal involvement.When Ground Glass opacities are severe 50–75 % of pulmonary parenchymal involvement is seen with pulmonary consolidation, and ≥ 75% of pulmonary parenchymal involvement is seen in critical cases with disseminated GGO with consolidation.

3.2 System Methodology

This work emphasizes quantum convolution for feature extraction and uses a stripe-based integration strategy to alleviate noise-free qubit limitations. The hybrid technique integrates classical fully connected layers with parameterized quantum circuits to improve image classification by merging quantum and classical computing models.
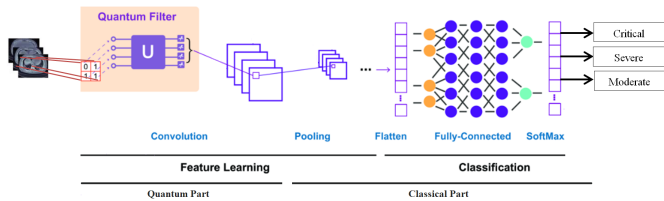
Figure 3: Hybrid Quantum-Classical Model
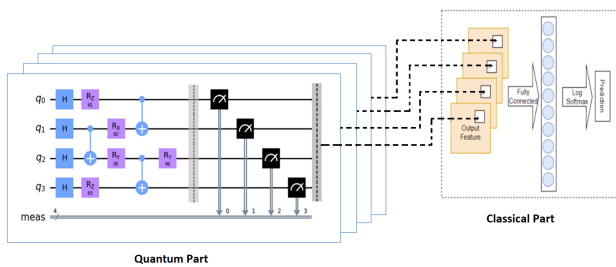
Figure 4: Four Qubit Quantum-Convolution Model

The following is a list of steps that this hybrid quantum-classical model goes through.

1. The dataset images are reduced in size to 28*28, 32*32, and 64*64 pixels, respectively, based on the requirements of the experiment. In the preprocessing stage, the training dataset was standardized using the mean and standard deviation of the training dataset to expedite the convergence of the training model.In this case, the standard deviation is [0.4143, 0.4143, 0.4143], while the mean is [0.5160, 0.5160, 0.5160].

2. The quantum convolutional layer collects 2x2 strips of input images, yielding identical-sized quantum qubits initially in the base state. Parameterized quantum circuits, utilizing CNOT gates and gates like Rz, Rx, Ry, along with Hadamard gates for superposition, facilitate unitary transformations, followed by correlation-based measurements to yield scalar outputs.

3. Via pooling, lowering the feature maps spatial dimensionality. When just one qubit out of the four is measured, qubit selection with classical post-processing pooling is used.Qubit, can be randomly selected for each iteration of the calculation.Classical post-processing methods are employed to evaluate measurement outcomes, get relevant data, and enhance the information obtained from the random qubit through feature extraction and dimensionality reduction.

4. Using non-linear activation functions and flattening into a 1D array, post-processing in classical approaches decreases computing cost, enhances feature translation invariance, and manages overfitting.After that, it flattens and moves through the fully connected layer, where it is processed further. Since it is a component of a classical neural network, additional classical neural network operations are also carried out.The output layer uses probabilities to determine class classification and makes use of the softmax activation function.

5. The fully connected layer's weights and the trainable quantum filter's parameters are adusted by implementing the Adam optimizer and Categorical Cross Entropy loss functions.Subsequently. The classification process then uses the ultimate stable model.

3.3 Evaluation Index

Effectiveness appears to be a determining factor in every machine learning model's prediction accuracy.The efficacy is evaluated from the proposed model using the following performance evaluation metrics.

$$\text{Accuracy} = \frac{(TP + TN)}{(TP + TN + FP + FN)} \quad (11)$$

$$\text{Specificity} = \frac{TN}{(TN + FP)} \quad (12)$$

$$\text{Precision} = \frac{(TP)}{(TP + FP)} \qquad (13)$$

$$\text{Recall} = \frac{(TP)}{(TP + FN)} \qquad (14)$$

$$\text{F-measure} = 2 \times \frac{(\text{precision} \times \text{Recall})}{(\text{Precision} + \text{Recall})} \qquad (15)$$

Where, **TP** (True Positive), **TN** (True Negative), **FN** (False Negative), and **FP** (False Positive) represents as COVID-19 severity correctly classify.

4. Result and Discussion

4.1 Experimental Setup

A hybrid Quantum-Classical model based on Computed Tomography (CT) scans is utilized to classify COVID-19 severity using PennyLane and PyTorch. TPU runtime is used to run the model on Google Colab. A qubit simulator is utilized in its place since a quantum computer is not feasible.The quantum variational circuit is drawn using the Qiskit framework.This experiment was carried out in the Google Colab Pro Plus edition, which has a runtime of up to 24 hours and has background execution capabilities that neither Google Colab Free nor Google Colab Pro do.The following are Google Colab Pro Plus's features:- Resources guarantee: High Percentage, Processor: 52 GB of RAM, GPU (K80, T4, and P100) and TPU, Run Time: 24 hours ,Targeted Class :High-performance computing user.

A hybrid Quantum-Classical model is used to accomplish the classification problem.In hybrid Quantum-Classical models, the number of quantum depths used to train the model remains constant.The model's hyper-parameters consist of an epoch-number varying learning rate of 0.0001, a 64-batch size, and an Adam optimizer with a categorical cross-entropy loss function.In this task, these models are able to classify the chest CT images severity into three categories: Critical, Severe, and Moderate.Table 1 shows the data used for classification. The entire data for classification is split in a ratio of 70:30, with 2780 pictures used for training and 1195 images used for testing. In the same way, a split of 75:25 is employed for the total 11050 photos used for deep learning comparison.

4.2 Comparison of Accuracy curve obtains from Training Vs Validation of different architectures

For both models, the training and validation datasets contain images from three separate classes. For VGG-19, batch size 32 is taken into consideration, while for quantum-classical, batch size is 64 . Different sizes of images have been used in quantum-classical training with varying epoch numbers to get varying accuracy values with varying run times using the same dataset.After 10 epoches, learning rate becomes adaptive.In a similar manner, VGG-19 achieves its accuracy at 64 by 64 image size and 150 epoch number.

Figure 5: Training Vs Validation: Using an image size of 28*28, the Quantum-Classical architecture is run for 11 epochs, and

Table 2: Training Vs Validation Accuracy of models

Model	Img. size	Epo.	Param.	Run(Min)	Acc.
Q-C	28*28	11	2355	812	95.31 %
Q-C	32*32	11	3075	1295	96.82 %
Q-C	64*64	4	12291	1234	92.04 %
VGG-19	64*64	150	262659	16	85.97 %

the graph validates an accuracy of 95.31%. Figure 6: Training Vs Validation runs using a 32*32 image size across 11 epochs utilizing a Quantum-Classical architecture. The graph validates an accuracy of 96.82%.
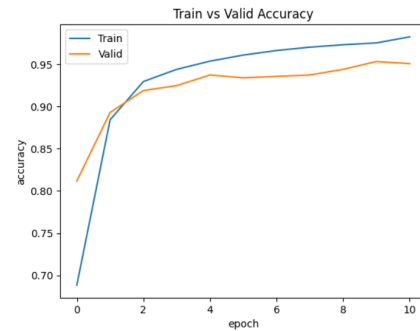

Figure 5: Training Vs Validation Accuracy based on Quantum-Classical model of 28*28
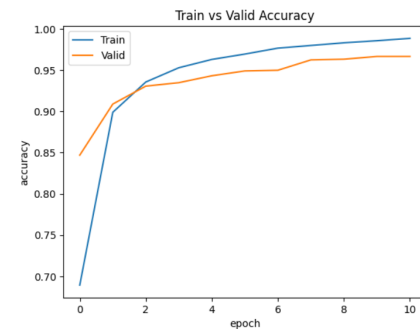

Figure 6: Training Vs Validation Accuracy based on Quantum-Classical model of 32*32

Figure 7: Training Vs Validation runs using a 64*64 image size across 4 epochs utilizing a Quantum-Classical architecture; the graph validates an accuracy of 92.04%. Figure 8: Training Vs Validation runs Using a 64*64 image and 150 epochs of VGG-19 architecture, the graph validates an accuracy of 85.97%.

4.3 Comparison of Loss curve obtains from Training Vs Validation of different architectures

Figure 9: Training Vs Validation runs using a 28*28 image size across 11 epochs utilizing a Quantum-Classical architecture, the graph validates the loss of 16.93%. Figure 10: Training Vs Validation: Using a 32*32 image across 11 epochs of Quantum-Classical architecture, the graph validates the loss of 15.10%.

Figure 11 :Training Vs Validation run using image size 64*64 for 4 epochs utilizing Quantum-Classical architecture , the graph validate the loss of 24.41%. Figure 12: Training Vs Validation run using image size 64*64 for 150 epochs utilizing VGG-19 architecture, the graph validate the loss of 41.00%.
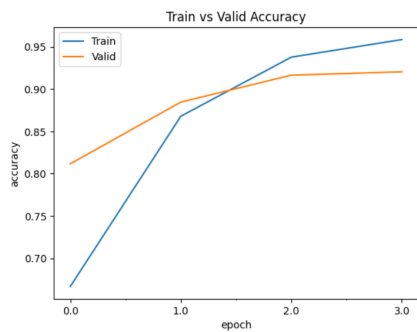
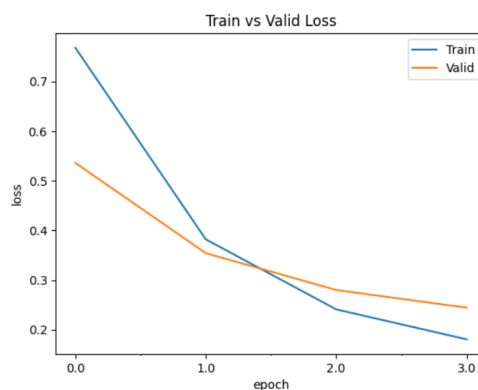**Figure 7:** Training Vs Validation Accuracy based on Quantum-Classical model of 64*64

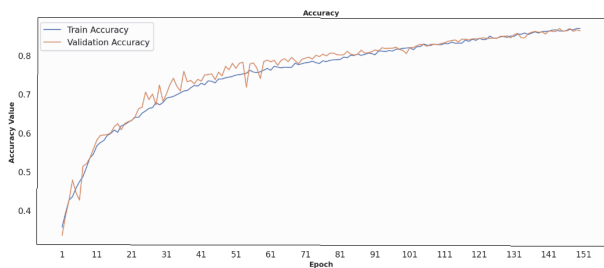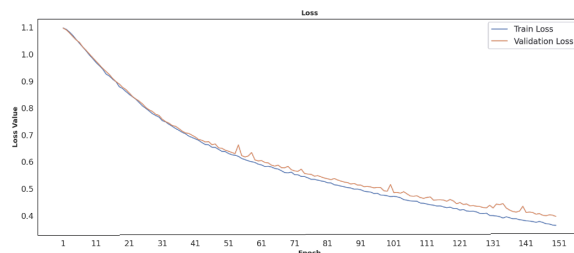**Figure 8:** Training Vs Validation Accuracy based on VGG-19 model of 64*64

Figure 9: Training Vs Validation Loss based on Quantum-Classical model of image 28*28

Figure 10: Training Vs Validation Loss based on Quantum-Classical model of image 32*32

Figure 11: Training Vs Validation Loss based on Quantum-Classical model of of image size 64*64

Figure 12: Training Vs Validation Loss based on VGG-19 model of image size 64*64
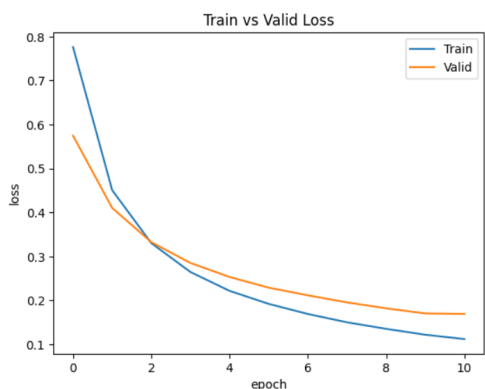
4.4 Comparison of ROC curve of different architectures

Figure 13 shows a ROC curve using a Quantum-Classical architecture run for 11 epochs, utilizing a 28 x 28 image size with an AUC score of 1.0 for critical, 0.99 for severe, and 0.99 for moderate. Figure 14 shows a ROC curve using a Quantum-Classical architecture that was ran for 11 epochs utilizing a 32 by 32 image size with an AUC score of 1.0 for critical, 1.0 for severe, and 0.99 for moderate.
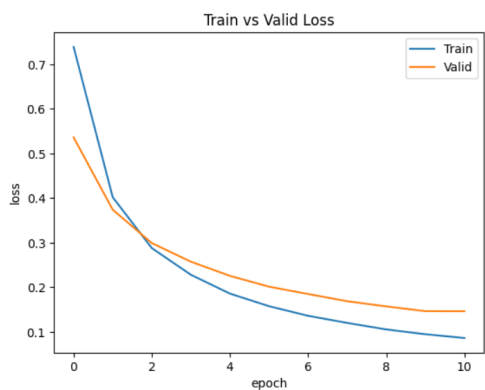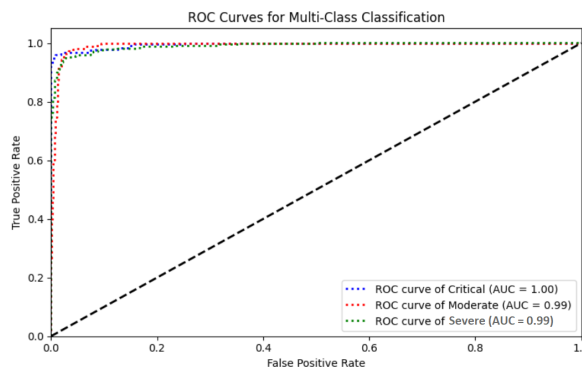

Figure 13: ROC curve based on Quantum-Classical model using image size of 28*28

Figure 15 shows a ROC curve using a Quantum-Classical architecture run for 4 epochs, utilizing a 64 * 64 image size with an AUC score of 0.95 for critical, 0.92 for severe, and 0.92 for moderate. Figure 16 shows a ROC curve using a VGG-19 architecture that was ran for 150 epochs utilizing a 64 * 64
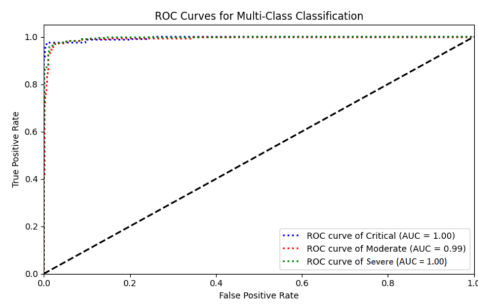
Figure 14: ROC curve based on Quantum-Classical model using image size of 32*32

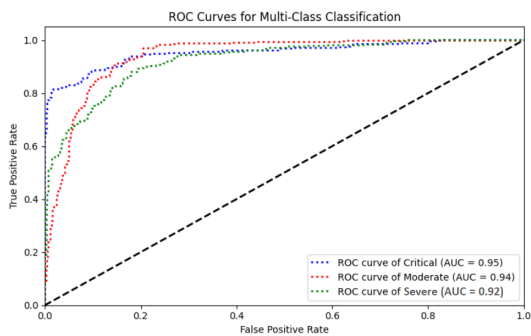image size with an AUC score of 0.92 for critical, 0.84 for severe, and 0.92 for moderate.

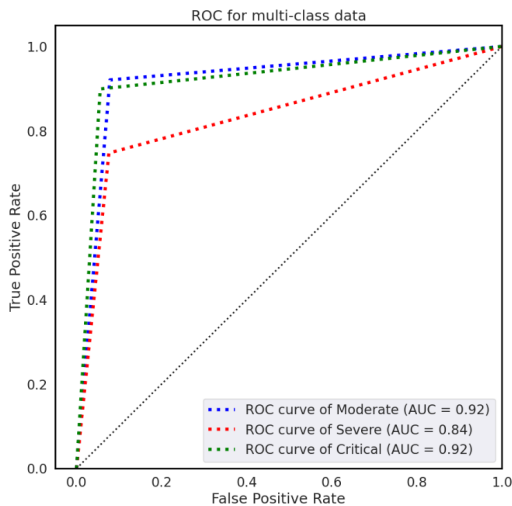**Figure 15:** ROC curve based on Quantum-Classical model using image size of 64*64

Figure 16: ROC curve based on VGG-19 model using image size of 64*64

4.5 Comparison of Confusion Matrix of different architectures

Figure 17 shows Confusion Matrix, run for 11 epochs with Quantum-Classical architecture using image size 28*28 whose model accuracy is 95.31% and loss is 16.93%.Figure 18 shows Confusion Matrix, run for 11 epochs with Quantum-Classical architecture using image size 32*32 whose model accuracy is 96.82% and loss is 15.10%.
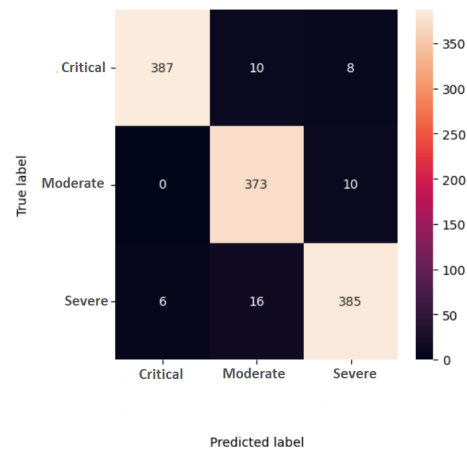

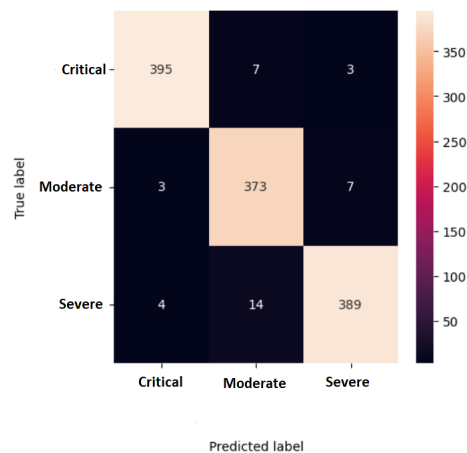**Figure 17:** Confusion matrix based on Quantum-Classical model using image size of 28*28

Figure 18: Confusion matrix based on Quantum-Classical model using image size of 32*32

Figure 19 shows Confusion Matrix, run for 4 epochs with Quantum-Classical architecture using image size 64*64 whose model accuracy is 92.04% and loss is 24.41%.Figure 20 shows Confusion Matrix, run for 150 epochs with VGG-19 architecture whose model accuracy is 85.97% and loss is 41.00%.

4.6 Discussion

The experiment compares Quantum-Classical and VGG-19 models for severity classification using a dataset of 3975 images. Quantum-Classical achieves accuracy rates of 95.31%, 96.82%, and 92.04% for image sizes of 28*28, 32*32, and 64*64, respectively, while VGG-19 achieves 85.97% accuracy. A Quantum-Classical system is shown to be able to learn its fundamental characteristics and representations of objects and patterns seen in higher-resolution images can still be captured by features taken from low-resolution images. This shows that the concepts of quantum advantage, robustness, and interpolation. Therefore, the representations learned on low-resolution images may generalize to larger images. To solve scaling issues and verify applicability in real-world circumstances, validation on larger images is essential. Although quantum computing has only been explored on
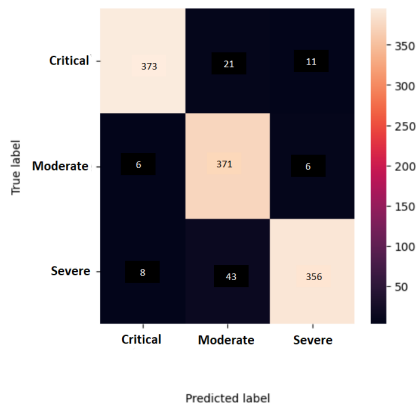
Figure 19: Confusion matrix based on Quantum-Classical model using image size of 64*64
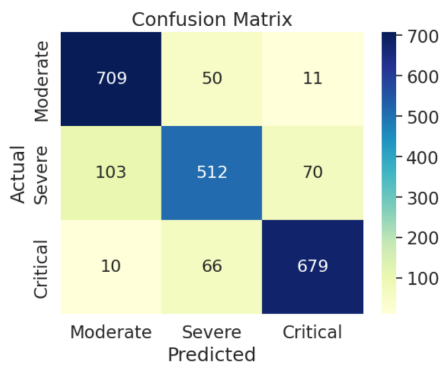

Figure 20: Confusion matrix based on VGG-19 model using image size of 64*64

low-resolution images, it has potential advantages for image processing applications. Its capacity to take use of quantum concepts like as superposition and entanglement can result in exponential acceleration in specific tasks, indicating improved performance for pattern recognition and image processing even in the case of low-resolution inputs. However, further research and development are needed to fully harness its capabilities for higher-resolution images. To model quantum circuits with the Cirq simulator, PennyLane was utilized as an interface. With Cirq serving as the backend for simulation or execution, PennyLane offers a higher-level interface for activities related to quantum computing.Testing with a single filter across different input sizes evaluates their impact on execution time and performance. Uniformly, one filter was applied for all input sizes to assess consistency.

The model's parameters affected the overall complexity, increasing in direct proportion to the amount of the input.Due to a significant increase in execution time for the 64*64 input size, the model was trained for a restricted number of epochs in order to appropriately manage computing resources.The classical model needed less time to train than the quantum model. Because the local simulator had to imitate the quantum model, this prolonged the training duration. When one simulates a quantum computer in a classical environment, the level of complexity increases exponentially. The larger image, the longer the training period and the more

parameters used.

VGG-19's deep structure and large number of parameters make it prone to overfitting when used for comparison with small image sizes, such as 32*32. There are spatial errors, indicating that it's not the best for such low resolution images . At 64*64 image size, VGG-19 shows a large loss and just a slight gain in accuracy, suggesting performance constraints at smaller dimensions.The shortcoming of the proposed model,near-term quantum devices are employed due to their capacity for small quantum circuits, aligning with available qubit. Quantum kernels in image processing induce resolution downsampling while maintaining image contours, contrasting classical convolution layers mainly quantum model perform on MNIST dataset .The HQ Hybrid Model's small design makes it ineffective for handling massive datasets.
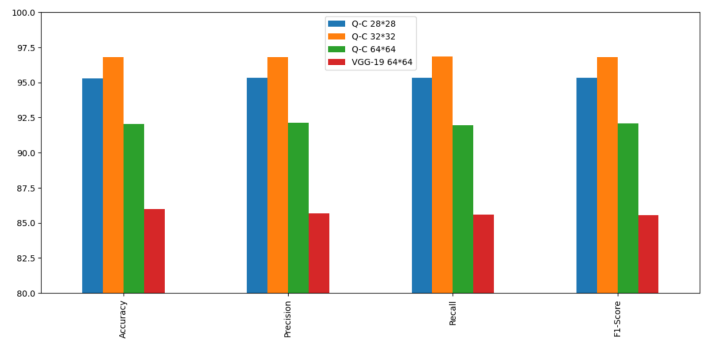

Figure 21: Comparison of Classification reports of quantum-classical and VGG-19

Comparison of similar works

Table 3: Different reference paper with similar works

Paper	Dataset	Method	ACC.	AUC.
[3]	956 samples	Random Forest (RF)	90.95%	-
[4]	176 samples	Random Forest (RF)	87.5%	-
[6]	825 samples	QTL	84%	-
[7]	6426 samples	Hybrid QC	93.48%	-
[17]	8768 samples	CQ	99%	-
Proposed	3975 samples	Hybrid QC	95.31% (28*28) 96.82% (32*32) 92.04% (64*64)	0.993 0.997 0.936

Table 3 presents a comparison of the Severity Classification based on similar research and many reference publications. In order to reach 84 % accuracy, V. Azevedo et al. [10] employed 825 CT scans for their model QTL. With 6426 X-ray images, the Hybrid QC model [7] was applied in given article, producing an accuracy of 93.48%. Umer et al. [17] used Classical Quantum to achieve 99% accuracy on 8,768 sample images.

5. Conclusion and Future work

This work presents a novel approach to the classification of lungs severity CT scans using a hybrid Quantum-Classical model, separating COVID-19 severity into three groups: moderate, severe, and critical. With the use of quantum convolution filters on 28*28, 32*32, and 64*64 resolutions of chest CT images, the research proposes a COVID-19 severity quantification model for timely medical assessments. Despite CNNs' effectiveness as feature extractors, the hybrid Quantum-Classical model outperforms them with an accuracy of 96.82% for a 32*32 input and 2*2 quantum filter. However, testing with a 64*64 image size yields a little lower accuracy of 92.04% due to execution time restrictions. More image datasets and higher resolutions may be able to increase accuracy even more, establishing a proportionate relationship between computing efficiency and model performance. Quantum convolution with a higher dimensional quantum filter applied. While some of the hyperparameters in this study may have been adjusted, most of them were left unchanged. Furthermore, the creation of intricate hybrid Quantum-Classical variational algorithms may benefit from this paradigm in the future. In future work on improving the method and work on Imagenet like dataset and improve in architecture to handle large datasets. In the future, this work may be further investigated to distinguish between various diseases and the lung region that is impacted.

Acknowledgments

References

[1] Ahmad Imwafak Alaiad, Esraa Ahmad Mugdadi, Ismail Ibrahim Hmeidi, Naser Obeidat, and Laith Abualigah. Predicting the severity of covid-19 from lung ct images using novel deep learning. *Journal of medical and biological engineering*, 43(2):135–146, 2023.

[2] Covid-19 coronavirus pandemic, 2024.

[3] Nasrin Amini and Ahmad Shalbaf. Automatic classification of severity of covid-19 patients using texture feature and random forest based on computed tomography images. *International Journal of Imaging Systems and Technology*, 32(1):102–110, 2022.

[4] Zhenyu Tang, Wei Zhao, Xingzhi Xie, Zheng Zhong, Feng Shi, Jun Liu, and Dinggang Shen. Severity assessment of coronavirus disease 2019 (covid-19) using quantitative features from chest ct images. *arXiv preprint arXiv:2003.11988*, 2020.

[5] Essam H Houssein, Zainab Abohashima, Mohamed Elhoseny, and Waleed M Mohamed. Hybrid quantum-classical convolutional neural network model for covid-19 prediction using chest x-ray images. *Journal of Computational Design and Engineering*, 9(2):343–363, 2022.

[6] Ubaid Ullah, Danyal Maheshwari, Hanna Helene Gloyna, and Begonya Garcia-Zapirain. Severity classification of covid-19 patients data using quantum machine learning approaches. In *2022 International Conference on Electrical, Computer, Communications and Mechatronics Engineering (ICECCME)*, pages 1–6. IEEE, 2022.

[7] Anish Baral. *Hybrid Quantum-Classical Deep Learning model for prediction of COVID-19 using CHEST X-RAY images*. PhD thesis, IOE Pulchowk Campus, 2022.

[8] Matthew Hayward. Quantum computing and shor's algorithm. *Sydney: Macquarie University Mathematics Department*, 1, 2008.

[9] Christof Zalka. Grover's quantum searching algorithm is optimal. *Physical Review A*, 60(4):2746, 1999.

[10] Vanda Azevedo, Carla Silva, and Inês Dutra. Quantum transfer learning for breast cancer detection. *Quantum Machine Intelligence*, 4(1):5, 2022.

[11] AL Aswathy, Hareendran S Anand, and SS Vinod Chandra. Covid-19 severity detection using machine learning techniques from ct-images. *Evolutionary Intelligence*, 16(4):1423–1431, 2023.

[12] Maxwell Henderson, Samriddhi Shakya, Shashindra Pradhan, and Tristan Cook. Quanvolutional neural networks: powering image recognition with quantum circuits. *Quantum Machine Intelligence*, 2(1):2, 2020.

[13] Mark Horowitz and Emily Grumbling. Quantum computing: progress and prospects. 2019.

[14] Mathurinache. Mosmeddata chest ct scans with covid-19. https://www.kaggle.com/datasets/mathurinache/mosmeddata-chest-ct-scans-with-covid19/data, Year of dataset publication or access. Kaggle Dataset.

[15] Sergey Morozov et al. Mosmeddata: Chest ct scans with covid-19 related findings, 2020.

[16] Daniel Bell, Ravi Sharma, Henry Knipe, et al. Covid-19. *Radiopaedia.org*, 2020. Accessed on 09 Apr 2024.

[17] Muhammad Junaid Umer, Javeria Amin, Muhammad Sharif, Muhammad Almas Anjum, Faisal Azam, and Jamal Hussain Shah. An integrated framework for covid-19 classification based on classical and quantum transfer learning from a chest radiograph. *Concurrency and Computation: Practice and Experience*, 34(20):e6434, 2022.